

Switchable Intermolecular Communication in a Four-Fold Rotaxane**

Yasuyuki Yamada, Mitsuhiro Okamoto, Ko Furukawa, Tatsuhisa Kato, and Kentaro Tanaka*

In biological systems, precise intermolecular electronic communication occurs in, and is regulated by, proteins and their complexes. For example, light-harvesting complexes have metal ions or metal complexes, such as manganese clusters, and organic cofactors, such as chlorophylls, carotenoids, or ubiquinones, in the “right” spatial arrangement so that electrons and energy can be efficiently transferred.^[1,2] Electronic communication between molecules is sensitive to their relative orientation. Large molecular scaffolds of proteins provide precise frameworks for molecular arrays as well as the ability of dynamic switching intermolecular communication, accomplished by conformational changes induced by external stimuli. These natural molecular frameworks are programmed as sequences of amino acids, but we could achieve flexible intermolecular communication in a simpler molecular architecture by using mechanically interlocked supramolecular motives, such as catenanes and rotaxanes, in which two or more molecular components are inseparable but their interactions are flexibly convertible.^[3,4] Syntheses of rotaxanes have been well-established, and a large variety of

fascinating examples of rotaxane-based molecular systems has been reported.^[3–5] As a specific example of switchable rotaxanes, Stoddart, Credi and co-workers reported elevator-like motion of a molecule with crown ethers along the strings on another molecule in a three-fold rotaxane, in which the relative position between the molecules was switchable by redox or acid-base reactions.^[6] Sauvage and co-workers made a porphyrin dimer in a cyclic [4]rotaxane and showed its ability to act as switchable receptor.^[7] Porphyrin, phthalocyanine, and their metal complexes have been applied to a broad range of functionalized molecular systems. Intermolecular electronic communication in their programmed arrays particularly has attracted a lot of interests in a wide range of fields, from photomaterials^[8] to pigments,^[9] molecular devices,^[10] and catalysts.^[11]

Herein, we report a mechanically linked cofacially stacked dimer of a metalloporphyrin and metallophthalocyanine units by formation of a four-fold rotaxane and its switchable spin–spin communication induced by external stimuli. A rotaxane consisting of a secondary ammonium ion and a crown ether has been recognized as a versatile building block for supramolecular systems. $R_2NH_2^+$ ions are complexed by dibenzo[24]crown-8 in a threaded manner as a result of electrostatic stabilization and hydrogen bonds between the negatively charged interior of the crown ether and the cationic ammonium moiety.^[12] We designed a porphyrin unit with four alkylammonium chains [**1**·4H]⁴⁺ and phthalocyanine unit with peripheral crown ethers **2** which are expected to form a facially stacked dimer through formation of a four-fold rotaxane (Figure 1).

The four-fold rotaxane [**3**·8H]⁴⁺·4Cl[−] was obtained in 41 % yield through formation of a pseudo-rotaxane between the porphyrin [**1**·5H]⁵⁺·5BARF[−] (BARF[−] = tetrakis[(3,5-bis-trifluoromethyl)phenyl]borate^[13]) and the phthalocyanine **2** in chloroform and acetone at a ratio of 4:1, followed by locking through Staudinger-phosphite reaction, which converts the azide groups to larger phosphoramidate units.^[14] The structure of the four-fold [2]rotaxane [**3**·8H]⁴⁺·4Cl[−] was given unambiguously by ESI-TOF mass spectrometry and NMR spectroscopy (Figure 2). The ESI-MS data clearly showed *m/z* values of 1365.0 (*z* = 3), 1377.0 (*z* = 3), and 1024.0 (*z* = 4), which confirmed the interlocked structure between [**1**·4H]⁴⁺ and **2** (calculated *m/z* values for [**3** + 7H]³⁺, [**3** + 8H + Cl]³⁺, and [**3** + 8H]⁴⁺ are 1365.0, 1377.0, and 1024.0, respectively; Figure 2b). The highly symmetric structure of [**3**·8H]⁴⁺·4Cl[−] was shown in the ¹H NMR spectrum (Figure 2a). All signals in the spectrum were assignable as one-quarter part of the four-fold rotaxane. Especially diagnostic are the high-field-shifted signals of the pyrrolic NH protons of both porphyrin and phthalocyanine units (H_a and H_α in Figure 2a, respectively), indicating a π–π stacking interaction and a close spatial arrangement between the crown ethers and the

[*] Dr. Y. Yamada, Prof. Dr. K. Tanaka
 Department of Chemistry, Graduate School of Science
 Nagoya University
 Furo-cho, Chikusa-ku, Nagoya 464-8602 (Japan)
 E-mail: kentaro@chem.nagoya-u.ac.jp

Dr. Y. Yamada
 Research Center for Materials Science, Nagoya University
 Furo-cho, Chikusa-ku, Nagoya 464-8602 (Japan)

M. Okamoto, Prof. Dr. T. Kato
 Department of Interdisciplinary Environment
 Graduate School of Human and Environmental Studies
 Kyoto University
 Yoshidanihonmatsu-cho, Sakyo-ku, Kyoto 606-8501 (Japan)

Dr. K. Furukawa
 Institute for Molecular Science
 Myodaiji, Okazaki 444-8585 (Japan)

Prof. Dr. T. Kato
 Institute for the Promotion of Excellence in Higher Education
 Kyoto University
 Yoshidanihonmatsu-cho, Sakyo-ku, Kyoto 606-8501 (Japan)

Prof. Dr. K. Tanaka
 CREST (Japan) Science and Technology Agency
 Honcho 4-1-8, Kawaguchi-shi, Saitama 332-0012 (Japan)

[**] We thank Dr. Miyo Yoshida of the chemical instrumentation facility, research center for materials science, Nagoya University for elemental analyses. This work was financially supported by the Grant-in-Aids for Scientific Research on the innovative area “Coordination Programming” (area 2107, grant number 21108012) and the global COE program for “Elucidation and Design of Materials and Molecular Functions” to K.T. from the Ministry of Education, Culture, Sports, Science, and Technology (Japan).



Supporting information for this article is available on the WWW under <http://dx.doi.org/10.1002/anie.201107104>.

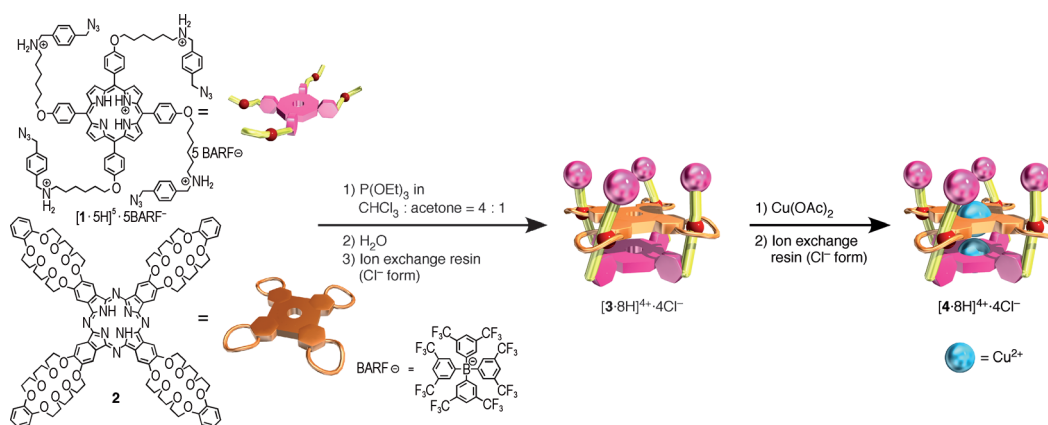


Figure 1. Self-assembly of the four-fold rotaxane and synthesis of its dinuclear Cu^{2+} complex. Formation of a pseudo-rotaxane between porphyrin **1** with alkyllammonium chains and phthalocyanine **2** with peripheral crown ethers, followed by locking through a Staudinger-phosphite reaction led to the formation of a four-fold rotaxane $[\mathbf{3}\cdot\mathbf{8H}]^{4+}\cdot\mathbf{4Cl}^-$. Reaction of $[\mathbf{3}\cdot\mathbf{8H}]^{4+}\cdot\mathbf{4Cl}^-$ with $\text{Cu}(\text{OAc})_2$ (2 equiv) yielded the dinuclear Cu^{2+} complex $[\mathbf{4}\cdot\mathbf{8H}]^{4+}\cdot\mathbf{4Cl}^-$.

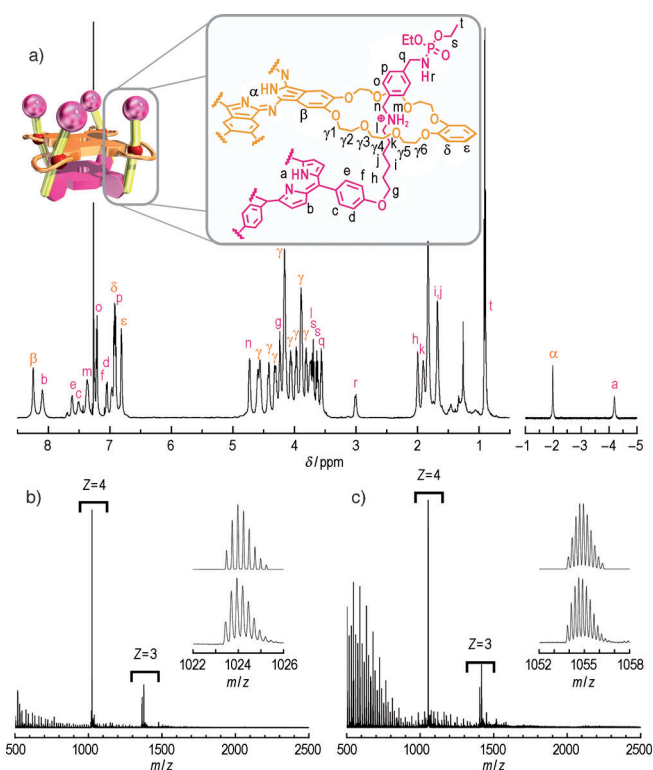


Figure 2. ^1H NMR (600 MHz) of the four-fold rotaxane $[\mathbf{3}\cdot\mathbf{8H}]^{4+}\cdot\mathbf{4Cl}^-$ in CDCl_3 at 293 K. The signals labeled with a–t (shown in pink) are assigned to the resonance of porphyrin **1** with alkyllammonium chains, and the signals labeled with α – ε (shown in orange) are assigned to the resonances of the phthalocyanine **2** with peripheral crown ethers. b) ESI-TOF MS spectra of $[\mathbf{3}\cdot\mathbf{8H}]^{4+}\cdot\mathbf{4Cl}^-$ (M for $[\mathbf{3}\cdot\mathbf{8H}]^{4+} = \text{C}_{220}\text{H}_{280}\text{N}_{20}\text{O}_{48}\text{P}_4$). c) ESI-TOF MS spectra of $[\mathbf{4}\cdot\mathbf{8H}]^{4+}\cdot\mathbf{4Cl}^-$ (M for $[\mathbf{4}\cdot\mathbf{8H}]^{4+} = \text{C}_{220}\text{H}_{276}\text{N}_{20}\text{O}_{48}\text{P}_4\text{Cu}_2$). In the insets of (b) and (c) the measured MS signals are compared with the calculated isotope distribution patterns of the corresponding charge of the molecular ions.

alkyllammonium chains, which was observed in a ROESY spectrum (see the Supporting Information). Consequently, the porphyrin and the phthalocyanine units stacked in a C_4 -

symmetric four-fold [2]rotaxane structure, in which all alkyllammonium chains were mechanically locked by the phosphoramidate moiety in each crown ring. To the best of our knowledge, this is the first example of a facially stacked heterodimer of porphyrin and phthalocyanine units.

Both metallized porphyrin and phthalocyanine units were obtained by using $\text{Cu}(\text{OAc})_2$ to yield a dinuclear Cu^{2+} complex $[\mathbf{4}\cdot\mathbf{8H}]^{4+}\cdot\mathbf{4Cl}^-$ in 93% yield as blackish-green crystals (Figure 1). The rotaxane $[\mathbf{4}\cdot\mathbf{8H}]^{4+}\cdot\mathbf{4Cl}^-$ has two types of acidic protons, which are located at the four ammonium moieties ($-\text{NH}_2^+$) and the four phosphoramidate moieties ($-\text{NHP}(\text{O})-$). To neutralize the protons, initially we chose 1,8-diazabicyclo[5.4.0]undec-7-ene (DBU) as a base, but the absorption spectrum of $[\mathbf{4}\cdot\mathbf{8H}]^{4+}\cdot\mathbf{4Cl}^-$ remained unchanged upon addition of DBU. However, addition of the stronger phosphazene base (P1-*t*Bu) caused significant changes in the UV/Vis absorption spectra of the dinuclear complex in CH_2Cl_2 (Figure 3). The addition of up to four equivalents of phosphazene base changed the spectrum only slightly (Figure 3b), but with further addition, above four equivalents, both Soret and Q bands gradually decreased with a well-defined isosbestic point at 698 nm (Figure 3c). The titration profile (Figure 3d) clearly showed a two-stage process. The two stages were identified in control experiments using model compounds. The first stage shows deprotonation of the phosphoramidate moiety ($-\text{NHP}(\text{O})-$ to $-\text{N}^-\text{P}(\text{O})-$), whereas the second stage shows deprotonation of the ammonium moiety ($-\text{NH}_2^+$ to $-\text{NH}-$; see the Supporting Information). The fully deprotonated spectrum reverted to that of $[\mathbf{4}\cdot\mathbf{8H}]^{4+}$ upon addition of trifluoroacetic acid. The change in absorbance at 684 nm upon successive addition of base and acid shows the reversibility of the protonation and deprotonation processes without decomposition of the complex (Figure 3e).

Continuous-wave electron paramagnetic resonance (CW-EPR) spectra of the dinuclear Cu^{2+} complex in a four-fold rotaxane structure, $[\mathbf{4}\cdot\mathbf{8H}]^{4+}$, and its deprotonated species, $[\mathbf{4}]^{4-}$, in a frozen dichloromethane solution were recorded at 10 K by a conventional X-band spectrometer (Figure 4a and c, respectively). The spectrum of the protonated $[\mathbf{4}\cdot\mathbf{8H}]^{4+}$ was well-simulated as a sum of two isolated doublet ($S = 1/2$) spins

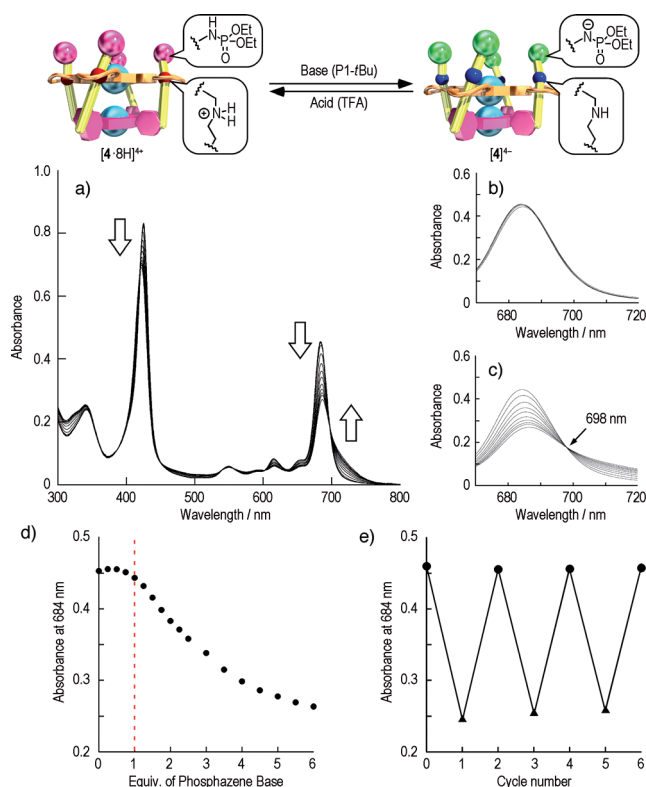


Figure 3. Photometric titration of the dinuclear copper complex $[4\cdot 8H]^{4+}\cdot 4Cl^-$ with the phosphazene base (P1-tBu). The dinuclear copper complex $[4\cdot 8H]^{4+}\cdot 4Cl^-$ was dissolved in CH_2Cl_2 at a concentration of 2.0×10^{-6} M at 293 K. a) The spectra change during addition of 0–24 equivalents of P1-tBu. b) The spectral change during addition of 0–4 equivalents of P1-tBu. c) The spectral change during the addition of 4–24 equivalents of P1-tBu (the isosbestic point is located at 698 nm). d) Plots of the absorbance at 684 nm. e) Reversible changes in the absorbance at 684 nm after successive addition of 40 equivalents of P1-tBu ($\bullet\rightarrow\Delta$) and 40 equivalents of trifluoroacetic acid ($\Delta\rightarrow\bullet$).

of Cu^{2+} centers in square-planar ligand fields of the porphyrin and phthalocyanine units without exchange interaction (Figure 4a). The signal intensities slightly increased with increasing temperature (Figure 4b). Since the profile was well-simulated by a Curie–Weiss model with $\theta = -1.0$ K, there is a very small antiferromagnetic mean-field interaction between the molecules. Spectra of the deprotonated $[4]^{4+}$ showed a pattern quite different from that of $[4\cdot 8H]^{4+}$ (Figure 4c). The spectrum of $[4]^{4+}$ showed a transition for $\Delta m_s = 1$ around 3000 Gauss with a fine structure arising from large zero-field splitting and a seven-lines hyperfine structure corresponding to two equivalents of copper atoms ($I = 3/2$) with spin exchange between the two Cu^{2+} centers. The forbidden transition at $\Delta m_s = 2$ was also observed around 1600 Gauss, accompanied by the seven lines of hyperfine structure because of the two equivalent copper atoms ($I = 3/2$). These features were well-reproduced in simulation. From the temperature dependence of the signal intensity (Figure 4d), the energy gap between the ground-state singlet and the first excited-state triplet was estimated to be only 7 K, and the Cu^{2+} – Cu^{2+} distance was estimated to be 4.06 Å by a point-charge approximation from the zero-field splitting parameter

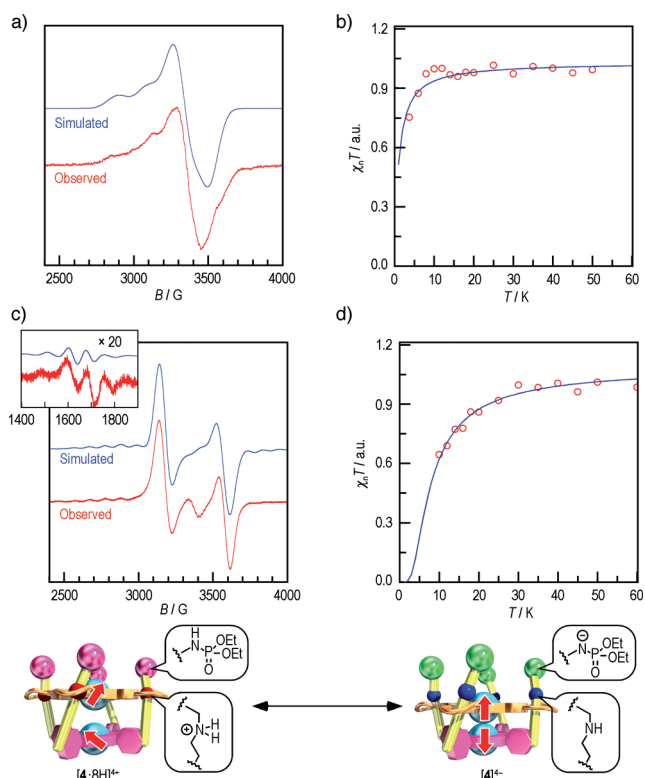


Figure 4. EPR spectra of the protonated and deprotonated forms of the dinuclear Cu^{2+} complex (B = magnetic field). a) Experimental (red curve) and simulated (blue curve) EPR spectra of the dinuclear copper complex $[4\cdot 8H]^{4+}\cdot 4Cl^-$ in the absence of the phosphazene base (P1-tBu) in CH_2Cl_2 at a concentration of 500 μ M at 10 K. b) Plots of $\chi_r T$ versus T for $[4\cdot 8H]^{4+}\cdot 4Cl^-$ in the absence of P1-tBu from $T = 4$ to 50 K. The blue curve shows the fit of $\chi_r T$ versus T for $[4\cdot 8H]^{4+}\cdot 4Cl^-$ using the Curie–Weiss model ($\theta = -1.0$ K). c) Experimental (red curve) and simulated (blue curve) EPR spectra of $[4\cdot 8H]^{4+}\cdot 4Cl^-$ in the presence of 8 equivalents of P1-tBu in CH_2Cl_2 at a concentration of 500 μ M at 10 K. The inset shows experimental (red) and simulated (blue) EPR spectra at the $\Delta m_s = 2$ transition in the half-field region. d) Plots of $\chi_r T$ versus T for $[4\cdot 8H]^{4+}\cdot 4Cl^-$ in the presence of 8 equivalents of P1-tBu from $T = 10$ to 60 K. The blue curve shows the fit of $\chi_r T$ versus T for $[4\cdot 8H]^{4+}\cdot 4Cl^-$ in the presence of 8 equivalents of the P1-tBu using a singlet–triplet model ($J/k_B = -7.0$ K).

($D = 41.8$ mT). Thus, antiferromagnetic coupling between Cu^{2+} –porphyrin and Cu^{2+} –phthalocyanine moieties was detected in the deprotonated form of the four-fold rotaxane. Although we obtained single crystals of the protonated dinuclear complex, we have not yet been able to perform crystallographic analysis because they are fragile. Nevertheless, the cofacial distance between porphyrin and phthalocyanine units in the protonated form is presumably longer than that in the deprotonated form, because the alkyl chain length between the porphyrin and the ammonium moiety was calculated to be about 9 Å, which is longer than the Cu^{2+} – Cu^{2+} distance in the deprotonated form and probably involves the inherent charge repulsion between the negatively charged interiors of the crown ethers and the lone pairs of the amine and phosphoramidate ions. In fact, a comparison of 1H NMR spectra of the free-base four-fold rotaxanes, protonated $[3\cdot 8H]^{4+}$, and deprotonated $[3]^{4+}$, showed significantly stron-

ger shielding effects in the signals of pyrrolic NH protons of the porphyrin and phthalocyanine units in $[3]^{4+}$. Consequently, the switchable spin-spin communication (isolated spins in the protonated form and antiferromagnetic coupling in the deprotonated form) is attributed to the variable distance of the two spin centers in the flexible four-fold rotaxane structure.

In summary, we have clearly shown switchable spin-spin communication between mechanically interlocked metal complexes induced by external stimuli. The spin-spin interactions are sensitively influenced by distance and relative spatial configuration between the Cu^{2+} centers. In comparison with biological templates such as proteins, the four-fold rotaxane has a symmetric and simpler design in which Cu^{2+} -porphyrin and Cu^{2+} -phthalocyanine moieties are, predictably, cofacially stacked and are able to change their spatial arrangements in response to external stimuli. The switching ability of the intermolecular communication could possibly extend from, for example the spin-spin interaction, reported in this work, to electron and energy transfer as well as catalytic reactions on metal centers. The number of ammonium moieties on each peripheral alkyl chain of the template porphyrin could be used to regulate the number of assembled phthalocyanines, yielding one-dimensional stacked phthalocyanine arrays. This concept would thus allow for preparation of well-defined molecular architectures with switchable functions related to nanomagnetism, conductivity, photonic properties, or catalysis. The development of programmable arrays of homogeneous and heterogeneous metal complexes in the rotaxane framework is now underway in our laboratory.

Experimental Section

Syntheses of $[1.5H]^{5+}$ -5BARF⁻ and **2** are provided in the Supporting Information.

Synthesis of the four-fold rotaxane $[3.8H]^{4+}$ -4Cl⁻: To an acetone solution (3.6 mL) of porphyrin $[1.4H]^{4+}$ -4BARF⁻ (107 mg, 18 μmol) a CHCl₃ solution (14.4 mL) of phthalocyanine **2** (38 mg, 18 μmol) was added. The resulting mixture was stirred at ambient temperature for 1 h, and then P(OEt)₃ (0.90 mL, 5.3 mmol) was added. After 73 h, the resulting solution was poured into a 1:1 mixture of hexane and Et₂O (100 mL). The blackish-green precipitate was collected by centrifugation and dissolved in MeOH (20 mL). Ion-exchange resin (IRA 400CJ (Cl⁻ form), 20 mL) was added to the solution to remove BARF⁻. After the resin was removed, the crude product was purified by silica gel column chromatography (2 cmφ × 21 cm, CHCl₃:MeOH = 4:1-1:1-CHCl₃:MeOH:H₂O:brine = 20:20:2:1). The fraction containing the desired product was washed with H₂O (50 mL × 3) and brine (50 mL × 2), dried over anhydrous Na₂SO₄, and concentrated under reduced pressure to give a blackish-green solid, which was dissolved in MeOH (10 mL) and treated with ion exchange resin (IRA 400 J CL (Cl⁻ form), 10 mL). Finally, recrystallization from CHCl₃:MeOH = 4:1/toluene/Et₂O yielded $[3.8H]^{4+}$ -4Cl⁻ as blackish-green needles (31 mg, 41%). ¹H NMR (600 MHz, CDCl₃/TMS): δ = 8.26 (br, 8H), 8.10 (br, 8H), 7.62 (br, 4H), 7.51 (br, 4H), 7.37 (br, 8H), 7.21 (d, *J* = 7.7 Hz, 8H), 7.05 (d, *J* = 7.3 Hz, 4H), 6.98 (br, 4H), 6.94-6.93 (m, 8H), 6.91 (d, *J* = 7.7 Hz, 8H), 6.82-6.81 (m, 8H), 4.73 (br, 8H), 4.60 (br, 8H), 4.57 (br, 8H), 4.42-4.41 (m, 8H), 4.32-4.31 (m, 8H), 4.24 (s, 8H), 4.16 (br, 24H), 4.07-4.04 (m, 8H), 3.99-3.96 (m, 8H), 3.90-3.89 (m, 16H), 3.81-3.79 (m, 8H), 3.79 (br, 8H), 3.74-3.62 (m, 16H), 3.55 (t, *J* = 8.2 Hz, 8H), 3.07-3.03 (m, 4H), 2.00 (br, 8H), 1.91 (br, 8H), 1.68 (br, 16H), 0.90 (t, *J* = 6.9 Hz, 24H),

-1.97 (br, 2H), -4.19 ppm (br, 2H). MS (ESI-TOF, positive) *m/z* 1024.0: calcd for C₂₂₀H₂₈₀N₂₀O₄₈P₄ ($[3.8H]^{4+}$), found: 1024.0. Anal. Calcd. for C₂₂₈H₃₀₄Cl₁₀N₂₀O₅₂P₄ ($[3.8H]^{4+}$ -4Cl⁻ + 2Et₂O + 2CHCl₃ + 2H₂O): C, 59.26; H, 6.62; N, 6.01. Found: C, 59.44; H, 6.73; N, 5.65. (0.36% Error).

Synthesis of dinuclear Cu²⁺ complex $[4.8H]^{4+}$ -4Cl⁻: The four-fold rotaxane $[3.8H]^{4+}$ -4Cl⁻ (12.3 mg, 2.9 μmol) and Cu(OAc)₂ (1.6 mg, 8.8 μmol) were dissolved in a 1:1 mixture of CHCl₃ and MeOH (3.0 mL) and the resulting solution was heated at 50 °C for 23 h. After the mixture was diluted with CHCl₃ (30 mL), it was washed with H₂O (50 mL × 3) and brine (50 mL), dried over anhydrous Na₂SO₄, and evaporated. The crude product was purified by silica gel column chromatography (2 cmφ × 10 cm, CHCl₃:MeOH = 4:1-1:1 and CHCl₃:MeOH:H₂O:brine = 10:10:2:1). The fraction containing the desired product was washed with H₂O (3 × 50 mL) and brine (2 × 50 mL), dried over anhydrous Na₂SO₄, and concentrated under reduced pressure to give blackish-green solid, which was dissolved in MeOH (20 mL) and treated with ion exchange resin (IRA 400 J CL (Cl⁻ form), 10 mL). Recrystallized from CHCl₃:MeOH = 9:1/toluene/Et₂O yielded $[4.8H]^{4+}$ -4Cl⁻ as blackish-green prism crystals (11.8 mg, 93%). MS (ESI-TOF, positive): *m/z* 1053.9: Calcd for C₂₂₀H₂₇₆Cu₂N₂₀O₄₈P₄ ($[M]^{4+}$), Found: 1053.9. Anal. Calcd. for C₂₃₀H₃₀₆Cl₁₀Cu₂N₂₀O₅₄P₄ ($[4.8H]^{4+}$ -4Cl⁻ + 2Et₂O + 2CHCl₃ + 4H₂O): C, 57.31; H, 6.40; N, 5.81. Found: C, 57.38; H, 6.56; N, 5.44. (0.37% Error).

EPR measurements and simulations: CW EPR measurements were performed at various temperatures from 4 to 60 K using a Bruker model ELEXES E380 X-band spectrometer equipped with an Oxford 900 cryostat. All samples were prepared in a concentration range of 0.1-1.0 mM and deaerated by freeze-and-thaw cycles before the EPR measurements. The EPR spectral simulation was performed with the MATLAB subroutine package EasySpin,^[15] distributed from <http://easyspin.org/>. The EPR simulation parameters were for the protonated $[4.8H]^{4+}$: the porphyrin site, spin quantum number: *S* = 1/2, *g* tensor: *g* = (2.047, 2.047, 2.186), hyperfine coupling (hfc) tensor of Cu nuclear spin: *A*_{Cu} = (3.0, 3.0, 21.0)/mT, hfc tensor of N nuclear spin: *A*_N = (2.0, 2.0, 2.0)/mT. The phthalocyanine site, spin quantum number: *S* = 1/2, *g* tensor: *g* = (2.059, 2.059, 2.157), hfc tensor of Cu nuclear spin: *A*_{Cu} = (1.7, 1.7, 20.0)/mT, hfc tensor of N nuclear spin: *A*_N = (1.86, 1.86, 1.86)/mT. For the deprotonated $[4]^{4-}$: spin quantum number: *S* = 1, *g* tensor: *g* = (2.034, 2.034, 2.098), hfc tensor of Cu nuclear spin: *A*_{Cu} = (1.25, 1.25, 10.8)/mT, spin-spin dipole interaction parameters: *D* = 41.8 mT, *E* = 0.0 mT.

Received: October 7, 2011

Published online: December 1, 2011

Keywords: copper · phthalocyanines · porphyrinoids · rotaxanes

- [1] R. E. Blankenship, *Molecular Mechanisms of Photosynthesis*, Blackwell Science, Oxford, UK, **2002**.
- [2] a) N. Nelson, A. Ben-Shem, *Nat. Rev. Mol. Cell Biol.* **2004**, *5*, 971-982; b) A. Ben-Shem, F. Frolow, N. Nelson, *Nature* **2003**, *426*, 630-635; c) Y. Umena, K. Kawakami, J.-R. Shen, N. Kamiya, *Nature* **2011**, *473*, 55-61.
- [3] J.-P. Sauvage, P. Gaspard, *From Non-Covalent Assemblies to Molecular Machines*, Wiley-VCH, Weinheim, **2010**.
- [4] a) J. F. Stoddart, *Chem. Soc. Rev.* **2009**, *38*, 1802-1820; b) L. Fang, M. A. Olson, D. Benítez, E. Tkatchouk, W. A. Goddard III, J. F. Stoddart, *Chem. Soc. Rev.* **2010**, *39*, 17-29.
- [5] a) A. Harada, A. Hashidzume, H. Yamaguchi, Y. Takashima, *Chem. Rev.* **2009**, *109*, 5974-6023; b) J. D. Crowley, S. M. Goldup, A.-L. Lee, D. A. Leigh, R. T. McBurney, *Chem. Soc. Rev.* **2009**, *38*, 1530-1541; c) D. Thibeault, J.-F. Morin, *Molecules* **2010**, *15*, 3709-3730; d) K. D. Hänni, D. A. Leigh, *Chem. Soc. Rev.* **2010**, *39*, 1240-1251.

- [6] a) J. D. Badjić, C. M. Ronconi, J. F. Stoddart, V. Balzani, S. Silvi, A. Credi, *J. Am. Chem. Soc.* **2006**, *128*, 1489–1499; b) J. D. Badjić, V. Balzani, A. Credi, S. Silvi, J. F. Stoddart, *Science* **2004**, *303*, 1845–1849.
- [7] a) J. Frey, C. Tock, J.-P. Collin, V. Heitz, J.-P. Sauvage, *J. Am. Chem. Soc.* **2008**, *130*, 4592–4593; b) J.-P. Collin, J. Frey, V. Heitz, J.-P. Sauvage, C. Tock, L. Allouche, *J. Am. Chem. Soc.* **2009**, *131*, 5609–5620; c) J.-P. Collin, F. Durola, V. Heitz, F. Reviriego, J.-P. Sauvage, Y. Trolez, *Angew. Chem.* **2010**, *122*, 10370; *Angew. Chem. Int. Ed.* **2010**, *49*, 10172–10175; d) J.-P. Collin, F. Durola, J. Frey, V. Heitz, F. Reviriego, J.-P. Sauvage, Y. Trolez, K. Rissanen, *J. Am. Chem. Soc.* **2010**, *132*, 6840–6850; e) J.-P. Sauvage, Y. Trolez, D. Canevet, M. Sallé, *Eur. J. Org. Chem.* **2011**, 2413–2416.
- [8] S. Fukuzumi, T. Honda, K. Ohkubo, T. Kojima, *Dalton Trans.* **2009**, 3880–3889.
- [9] N. Aratani, D. Kim, A. Osuka, *Acc. Chem. Res.* **2009**, *42*, 1922–1934.
- [10] S. Mohnani, D. Bonifazi, *Coord. Chem. Rev.* **2010**, *254*, 2342–2362.
- [11] S. J. Lee, S. Cho, K. L. Mulfort, D. M. Tiede, J. T. Hupp, S. T. Nguyen, *J. Am. Chem. Soc.* **2008**, *130*, 16828–16829.
- [12] a) P. R. Ashton, P. J. Campbell, E. J. T. Chrystal, P. T. Glink, S. Menzer, D. Philp, N. Spencer, J. F. Stoddart, P. A. Tasker, D. J. Williams, *Angew. Chem.* **1995**, *107*, 1997–2001; *Angew. Chem. Int. Ed. Engl.* **1995**, *34*, 1865–1869; b) P. R. Ashson, M. C. T. Fyfe, P. T. Glink, S. Menzer, J. F. Stoddart, A. J. P. White, D. J. Williams, *J. Am. Chem. Soc.* **1997**, *119*, 12514–12524; c) N. Watanabe, T. Yagi, N. Kihara, T. Takata, *Chem. Commun.* **2002**, 2720–2721; d) A. R. Williams, B. H. Northrop, K. N. Houk, J. F. Stoddart, D. J. Williams, *Chem. Eur. J.* **2004**, *10*, 5406–5421.
- [13] K. Fujiki, M. Kashiwagi, H. Miyamoto, A. Sonoda, *J. Fluorine Chem.* **1992**, *57*, 307–321.
- [14] W. Hung, K. Liao, Y. Liu, S. Peng, S. Chiu, *Org. Lett.* **2004**, *6*, 4183–4186.
- [15] S. Stoll, A. Schweiger, *J. Magn. Reson.* **2006**, *178*, 42–55.